Journal of Alzheimer's Disease 98 (2024) 1001–1016
DOI 10.3233/JAD-231153
IOS Press

Low-Dose Radiation Therapy Impacts Microglial Inflammatory Response without Modulating Amyloid Load in Female TgF344-AD Rats

Kelly Ceyzériat[a,b,c,d,*], Emma Jaques[a,b], Yesica Gloria[a,b,e], Aurélien Badina[a,b], Philippe Millet[a,b], Nikolaos Koutsouvelis[f], Giovanna Dipasquale[f], Giovanni B. Frisoni[b,c], Thomas Zilli[b,f,g,h], Valentina Garibotto[b,c,d] and Benjamin B. Tournier[a,b]

[a]*Department of Psychiatry, University Hospitals of Geneva, Geneva, Switzerland*
[b]*Faculty of Medicine, Geneva University, Geneva, Switzerland*
[c]*Diagnostic Department, Division of Nuclear Medicine and Molecular Imaging, Geneva University Hospitals and NIMTLab, Faculty of Medicine, Geneva University, Geneva, Switzerland*
[d]*CIBM Center for BioMedical Imaging, Faculty of Medicine, University of Geneva, Geneva, Switzerland*
[e]*Bertarelli Foundation Gene Therapy Platform, School of Life Sciences, Ecole Polytechnique Fédérale de Lausanne (EPFL), Geneva, Switzerland*
[f]*Department of Oncology, Division of Radiation Oncology, Geneva University Hospitals, Geneva, Switzerland*
[g]*Department of Radiation Oncology, Oncology Institute of Southern Switzerland, EOC, Bellinzona, Switzerland*
[h]*Facoltà di Scienze Biomediche, Università della Svizzera Italiana, Lugano, Switzerland*

Accepted 2 February 2024
Pre-press 12 March 2024

Abstract.
Background: Low-dose radiation therapy (LD-RT) has demonstrated in preclinical and clinical studies interesting properties in the perspective of targeting Alzheimer's disease (AD), including anti-amyloid and anti-inflammatory effects. Nevertheless, studies were highly heterogenous with respect to total doses, fractionation protocols, sex, age at the time of treatment and delay post treatment. Recently, we demonstrated that LD-RT reduced amyloid peptides and inflammatory markers in 9-month-old TgF344-AD (TgAD) males.
Objective: As multiple studies demonstrated a sex effect in AD, we wanted to validate that LD-RT benefits are also observed in TgAD females analyzed at the same age.
Methods: Females were bilaterally treated with 2 Gy × 5 daily fractions, 2 Gy × 5 weekly fractions, or 10 fractions of 1 Gy delivered twice a week. The effect of each treatment on amyloid load and inflammation was evaluated using immunohistology and biochemistry.
Results: A daily treatment did not affect amyloid and reduced only microglial-mediated inflammation markers, the opposite of the results obtained in our previous male study. Moreover, altered fractionations (2 Gy × 5 weekly fractions or 10 fractions of 1 Gy delivered twice a week) did not influence the amyloid load or neuroinflammatory response in females.
Conclusions: A daily treatment consequently appears to be the most efficient for AD. This study also shows that the anti-amyloid and anti-inflammatory response to LD-RT are, at least partly, two distinct mechanisms. It also emphasizes the necessity to assess the sex impact when evaluating responses in ongoing pilot clinical trials testing LD-RT against AD.

Keywords: Alzheimer's disease, amyloid, low-dose radiation therapy, microglial response

*Correspondence to: Kelly Ceyzériat, PhD, CIBM Center for BioMedical Imaging, University of Geneva, Avenue de la Roseraie, 64, 1205 Geneva, Switzerland. Tel.: +41 22 379 46 56; E-mail: kelly.ceyzeriat@unige.ch.

INTRODUCTION

Alzheimer's disease (AD) is a neurodegenerative disease that affects mainly memory. Extracellular amyloid deposits, due to abnormal metabolism of amyloid-β (Aβ) peptides, has been the first hallmark of the disease described by Alois Alzheimer. Those peptides are produced after a successive cleavage of the amyloid-β protein precursor (AβPP) by the β-secretase (also named BACE1) and a γ-secretase. The non-amyloidogenic pathway, involving an α-secretase instead of BACE1, allows the production of a soluble AβPPα fragment, among others, which has been shown to be neuroprotective [1]. The amyloid deposits are accompanied by abnormal hyperphosphorylation of the tau protein, neuroinflammation, and degeneration of neurons. The neuroinflammatory phenomena correspond to the response of astrocytes and microglial cells, that become reactive to brain homeostasis dysregulation [2–4]. This reactive state is characterized for example by morphological and proteomic changes, with the upregulation of proteins such as GFAP and CD68 by astrocytes and microglia respectively.

Numerous risks factors have been identified, the most important being aging and sex with a higher incidence in women. The main hypothesis was initially that women generally live longer than men, reaching ages with higher risk to develop the pathology. However, growing evidence identifies sex hormones and estrogen dysregulation after menopause as specific disease modulators [5]. Despite this evidence, the sex effect in patient evaluation and treatment response is still generally under-evaluated and underreported in clinical studies [6].

Among the numerous therapeutical strategies developed against AD, low-dose radiation therapy (LD-RT) showed interesting results in animal models [7–13]. Indeed, this strategy could allow to decrease two central players in AD, namely amyloid load and neuroinflammation. A reduction of the tauopathy has also been suggested in a study [8], but the results were not replicated in younger mice in the same model [12]. Importantly, the evaluation of LD-RT efficiency varies between pre-clinical studies in terms of irradiation protocols, age and duration of treatment, delay post LD-RT and animal models. It is consequently difficult to correctly interpret results. In a recent study, we observed an efficient reduction of amyloid load and inflammation markers after a daily treatment with 2 Gray (Gy) delivered in 5 fractions in 9-month-old male TgF344-AD (TgAD) rats [14]. The same regimen led to spatial memory improvement in aged female TgAD without modification of amyloid load nor inflammation [10]. In another study on female 3xTg-AD mice, where we applied the same treatment at a pre-symptomatic stage, we only observed a decrease of highly aggregated $A\beta_{42}$ peptides and a trend to the reduction of other forms. Neuroinflammation markers studied were not impacted by LD-RT. Altogether, these results suggest a possible sex effect in the treatment response, with a lower sensitivity of females at the neurochemical level, which however has never been specifically investigated.

To verify this hypothesis, we treated female TgAD rats at the same age and with the same regimen than TgAD male rats, with 5 daily fractions of 2 Gy (Total dose: 10 Gy). As benign degenerative inflammatory pathologies are also commonly treated with lower fractionation protocols [15], we also evaluated other fractionations to compare their anti-inflammatory effect of LD-RT (5 once-a-week fractions of 2 Gy or 10 fractions of 1 Gy delivered twice a week; Total dose = 10 Gy) to the reference regimen.

MATERIAL AND METHODS

Animals

Female TgF344-AD rats harboring the human $APP_{swedish}$ and PS1dE9 transgenes on a Fisher 344 background [16] were treated at 9-month-old using different regimens of LD-RT and analyzed two-months later. Sham treated TgAD rats (sham) and sham treated non-transgenic littermates (wild type; WT) were used as controls. Animals were housed with food and water *ad libitum* in a 12-h light-dark cycle. Animals were randomly assigned to groups and tested in blind conditions (experimental treatment and genotype). All experimental procedures were approved by the Ethics Committee for Animal Experimentation of the Canton of Geneva, Switzerland.

Radiation treatment

Nine-month-old TgF344-AD rats received whole brain irradiation with a 6 MV direct radiation field under anesthesia (2% isoflurane) using a Truebeam® Linear Accelerator (Varian Medical Systems) as previously described [17]. The first cohort was treated with 5 daily fractions of 2 Gy (Total dose: 10 Gy; RT1, $n = 10$), the second cohort was treated with 5 once-a-week fractions of 2 Gy (Total dose: 10 Gy;

RT2, $n = 9$) and the third cohort was treated with 10 fractions of 1 Gy delivered twice a week for 5 weeks (Total dose: 10 Gy; RT3, $n = 11$). Sham treated TgAD animals ($n = 15$) and WT animals ($n = 15$) were randomly divided in the three cohorts ($n = 4$–6/cohort/genotype) and anesthetized accordingly. Animals were euthanized two months after the last treatment session.

Behavior

Alternative Y maze. The spatial working memory of animals assessed before treatment and 2 months after the last session of treatment using the alternative Y maze test. Rats were placed at the extremity of one arm of the device ($50 \times 50 \times 10$ cm) and video-tracked for 5 min. The number of good alternations between the 3 arms (success to the test) were automatically measured and analyzed using the EthoVision software (Noldus). Rats performing less than four entries during the session were excluded ($n = 16/58$).

Open field. This test was used to measure the general locomotion of animals before and after LD-RT. Rats were placed at the center of the square area ($45 \times 45 \times 40$ cm) and the total distance travelled was automatically measured during 1 h using a video tracking and EthoVision software.

Protein extraction

At the end of the behavioral session, animals were euthanized by decapitation under anesthesia. The brain was rapidly extracted, and the hemispheres were separated on ice. The half brain was dissected to collect the hippocampus and the frontal cortex, that were then snap frozen in liquid nitrogen. The rest of the cortex was also collected and snap frozen for mRNA analyses (see details below). Proteins were then extracted in a Triton X100 lysis buffer [50 mM Tris-HCl pH = 7.4, 150 mM NaCl, 1% Triton X-100 with 1× protease and phosphatase inhibitors (Pierce); 300 µl], centrifuged at 20,000 g for 20 min at 4°C. The supernatant contains Triton X100 (Tx)-soluble proteins. The pellet was re-suspended in a Guanidine lysis buffer [50 mM Tris-HCl pH = 8, 5 M Guanidine HCl with 1× protease and phosphatase inhibitors (Pierce); 180 µl], incubated for 3 h on ice and centrifuged at 20,000 g for 20 min at 4°C. The supernatant contains Guanidine (Gua)-soluble proteins. The total protein concentration was determined using the BCA test (Pierce). Manufacturer's protocol was followed.

ELISA tests

Aβ measurements. Different forms of Aβ peptides were measured using the following kits: human $A\beta_{40}$ ELISA test (Life Technologies), human $A\beta_{42}$ ELISA test (Life Technologies). Cortical Tx-soluble samples were diluted at 1/300 in the diluent buffer provide in $A\beta_{40}$ kit, and at 1/100 in the diluent buffer for $A\beta_{42}$. Gua-soluble samples were diluted at 1/16 in guanidine buffer and then at 1/500 in diluent buffer for $A\beta_{40}$; 1/800 in guanidine buffer and then at 1/500 in diluent buffer for $A\beta_{42}$. Hippocampal Tx-soluble samples were diluted at 1/10 in the diluent buffer of $A\beta_{40}$ kit, and at 1/250 in the diluent buffer for $A\beta_{42}$. Gua-soluble samples were diluted at 1/6 in guanidine buffer and then at 1/500 in diluent buffer for $A\beta_{40}$; 1/300 in guanidine buffer and then at 1/500 in diluent buffer for $A\beta_{42}$. Manufacturer's protocols were followed. Absorbances were measured at 450 nm using the EZ read 400 microplate reader (Biochrom). The absence of amyloid in WT was validated for all forms. Aβ concentrations were normalized to the total protein quantity (µg proteins).

sAβPPα and sAβPPβ measurements in the frontal cortex. Samples were diluted at 1/10 in the diluent provided in the ELISA kit of interest (Mybiosource). Manufacturer's protocols were followed. The absorbance was measured at 450 nm using the EZ read 400 microplate reader (Biochrom) and concentrations were normalized to the total protein quantity (µg proteins).

Western blot

After a denaturation step (70°C, 10 min) in a 1× Laemmli buffer/2.5% β-mercaptoethanol, 40 µg of proteins from the hippocampus or frontal cortex and a protein ladder (All blue precision plus ladder, Biorad) were loaded onto in Criterion™ TGX™ precast midi protein gel (Biorad) and migrated at 150 V for 55 min with the manufacturer's buffer (BioRad). Proteins were then transferred on a LF-PVDF membrane in 7 min at 2.5A constant, and up to 25 V in the manufacturer buffer using the Trans-blot Turbo machine (BioRad). Membrane was saturated in 5% non-fat dry milk/TBST (20 mM Tris, 150 mM NaCl, 0.1% Tween20, pH = 7.4) for 45 min and then incubated 48 h at 4°C with the following primary antibodies in 5% milk/TBST: CLUSTERIN (CLU; 1/250, mouse; R&D system), GFAP-Cy3 (1/250, mouse; Sigma), GAPDH (1/5000, rabbit; Cell signaling), SERPINA3 N (1/250, rabbit; Invitrogen), STAT3α

(1/250, rabbit; Cell signaling). After 3 washes in TBST of 10 min at room temperature, the membrane was immerged in the appropriated Alexa Fluor-conjugated secondary antibody (Alexa-Fluor 488 or 555; Invitrogen) in 5% milk/TBST for 90 min. After 3 washes in TBST (10 min, room temperature), the fluorescence was detected using the iBright imaging system (ThermoFisher Scientific). The same membrane was reused after a new saturation step. Densitometry analysis was performed using ImageJ to quantify proteins and protein levels were normalized to GAPDH levels.

Immunofluorescence

The other half brain of each animal was post fixed in 4% paraformaldehyde overnight (O/N) and cryoprotected with a sucrose solution before to be frozen in isopentane. Coronal slices (35 μm) were cut using a cryostat and stored at –20°C until use. After washes in PBS0.1M, slices were mounted on gelatin slides and let dry O/N. After rehydration in PBS0.1M, slices were incubated in 20 μg/ml methoxy-XO4 (MXO4; Tocris) in PBS0.1M for 30 min at room temperature to label amyloid plaques. Slices were rinsed in PBS0.1M and incubated O/N at 4°C with the following primary antibodies: anti-4G8 (1/500, Mouse; Biolegend), anti-GFAP-Cy3 (1/1000, Mouse; Sigma), anti-CD68 (1/1000, Rabbit; Invitrogen) in 1% BSA/PBS0.1M/0.3% Triton X-100. After 3 washes in PBS0.1M, slices were incubated for 1 h at room temperature in the appropriate secondary antibody (1/250, Alexa Fluor) in 1% BSA/PBS0.1M/0.3% Triton X-100. Finally, slices were rinsed before being coverslipped with Fluorosave™ (Calbiochem).

Image analyses

Images were acquired at 10× with the Axioscan.Z1 scanner (Zeiss) and analyzed using ImageJ. The hippocampal subregions (subiculum, dorsal, ventral) were manually delimited and an intensity threshold, kept constant between subregions, was applied to quantify the percentage of the region of interest (ROI) positively stained with MXO4, 4G8, or GFAP. For CD68, an intensity and size threshold, kept constant between subregions, were used to automatically count the number of $CD68^+$ cells, normalized by the size of the ROI. For correlation analyses of inflammation markers (GFAP or CD68) and amyloid plaques (MXO4 or 4G8), all groups were included as no differential effect was observed between TgAD groups.

RNA extraction and qPCR

Cortical samples were placed into 400 μl of Trizol. Samples were left at room temperature for 5 min and 1 volume of chloroform was added for 3 min. After a vortex and centrifugation at 12,000 g for 15 min at 4°C, the aqueous phase was collected and 1 volume of ethanol 70% was added. Samples were then transferred onto RNeasy columns (RNeasy micro kit, Qiagen) and the manufacturer's protocol was followed. RNA was eluted with 15 μl of nuclease free water. M-MLV reverse transcriptase synthesis kit (Invitrogen) with random primers (Promega) was used to synthesized cDNA as described by the manufacturer. Samples were diluted at 1/10 in H_2O and mixed with 250 nM of primers and PowerUp™ SYBR™ Green Master Mix (Applied Biosystems) for qPCR. The following sequences of primers were used: *Aif1-F:* CAGAGCAAGGATTTGCAGGGA, *Aif1-R:* CAAACTCCATGTACTTCGTCTTG; *Itgam-F:* CTTGGTGAAACCCGAGTGGT, *Itgam-R:* TCGATCGTGTTGATGCTACCG; *Trem2-F:* CCTGTGGGTCACCTCTAACC, *TREM2-R:* GGCCAGGAGGAGAAGAATGG; *Il1β-F:* CACACTAGCAGGTCGTCATCATC, *Il1β-R:* ATGAGAGCATCCAGCTTCAAATC; *Il6-F:* AGAGACTTCCAGCCAGTTGC, *Il6-R:* AGTCTCCTCTCCGGACTTGT; *Tnfα-F:* CAGAGCAATGACTCCAAAGTA, *Tnfα-R:* CAAGAGCCCTTGCCCTAA; *Tgf-β-F:* CCTGGAAAGGGCTCAACAC, *Tgf-β-R:* CAGTTCTTCTCTGTGGAGCTGA; *Il10-F:* GCAGTGGAGCAGGTGAAGAA, *Il10-R:* GTAGATGCCGGGTGGTTCAA; *Il4-F:* AGACGTCCTTACGGCAACAA, *Il4-R:* CACCGAGAACCCCAGACTTG; *Ppia-F:* ATGGCAAATGCTGGACCAAA, *Ppia-R:* GCCTTCTTTCACCTTCCCAAA. Undetermined Ct values were manually replaced by Ct = 40. Expression levels of genes of interest were normalized to the abundance of *Ppia* gene with the $2^{-\Delta\Delta Ct}$ method.

Statistics

Animals were randomly assigned to the different experimental groups. Analyses were performed in blind conditions and normality of residues was

assessed with the Shapiro-Wilks test. For the comparison of two groups, an unpaired *t*-test was performed. One-way ANOVA followed by a Tukey's multiple comparisons test or Kruskal-Wallis test followed by a Dunn's comparisons test, were used to compare more than two groups. Two-way ANOVA (Group and genes as between factors) and Tukey's multiple comparisons test were used to analyze qPCR data. Outliers were identified using the ROUT method (Maximal false discovery rate = 1%). All analyses were performed on GraphPad Prism 9.4.0. Statistical details are provided only if significance was reached.

RESULTS

A daily treatment did not decrease amyloid load in early AD females

Nine-month-old female TgAD were bilaterally treated with 5 consecutive fractions of 2 Gy delivered daily (named RT1 group in the rest of the manuscript; Fig. 1a). The effect of this regimen on different soluble or poorly aggregated Aβ peptides (Tx-soluble) and highly aggregated Aβ (Gua-soluble) was measured in the hippocampus and the frontal cortex of animals. LD-RT1 did not reduce Tx-soluble $A\beta_{40}$ and $A\beta_{42}$ (Fig. 1b, c) or Gua-soluble $A\beta_{40}$ and $A\beta_{42}$ (Fig. 1d, e) in the hippocampus of RT1-treated animals compared to sham-treated rats. Additionally, no effect on either of these Aβ peptides was observed in the frontal cortex (Fig. 1f–i). Using MXO4 and 4G8 antibody to label fibrillar dense-core [18] or both diffuse and dense-core plaques [19] respectively, we also quantified amyloid plaques in the hippocampal subregions. We can notice that the distribution of amyloid plaques was different within hippocampal subregions. Indeed, subiculum (Sub) showed higher plaques density ($MXO4^+$ and $4G8^+$) than the dorsal hippocampus (dH) or the ventral hippocampus (vH) in sham TgAD rats (Fig. 1j–l; MXO4: One-way-ANOVA, $F_{(1.064,8.509)} = 6.560$, $p = 0.0307$, Tukey's multiple comparisons test: $p = 0.1455$ Sub versus dH, $p = 0.0739$ Sub versus vH, $p = 0.0528$ dH versus vH; 4G8: One-way-ANOVA, $F_{(1.601,12.80)} = 16.41$, $p < 0.0001$, Tukey's multiple comparisons test: $p = 0.0403$ Sub versus dH, $p = 0.0032$ Sub versus vH, $p = 0.0180$ dH versus vH). However, LD-RT1 did not impact the plaque density in the different subregions (Fig. 1 m, n). The absence of modulation of soluble AβPPβ (sAβPPβ) levels in the frontal cortex (Fig. 1o) confirms that LD-RT1 did not impact any forms of the amyloid or the amyloidogenic pathway in females. To go further, we also quantified soluble AβPPα (sAβPPα) as index of the non-amyloidogenic pathway. The same levels of sAβPPα were quantified in RT1-treated and sham-treated groups (Fig. 1p).

A daily treatment reduced microglial inflammatory response in early AD females

The anti-inflammatory effect of LD-RT1 was first evaluated using classical markers of inflammation overexpressed by reactive astrocytes. In the frontal cortex, sham-treated TgAD rats did not show any difference compared to WT regarding GFAP, STAT3α, and sCLU (Fig. 2a–c and Supplementary Figure 1). SERPINA3 N levels appeared even decreased in both RT1-treated and sham-treated groups (Fig. 2d; One-way ANOVA, $F_{(2,22)} = 7.420$, $p = 0.0034$; Tukey's multiple comparisons test: $p = 0.0035$ WT versus sham, $p = 0.0344$ WT versus RT1, $p = 0.7265$ sham versus RT1). These results indicate that the pathology is not in place yet in this brain region. Only a significant increase of GFAP was measured after LD-RT1, suggesting a slight pro-inflammatory effect of the treatment (Fig. 2a; One-way ANOVA, $F_{(2,22)} = 9.514$, $p = 0.0011$; Tukey's multiple comparisons test: $p = 0.1426$ WT versus sham, $p = 0.0007$ WT versus RT1, $p = 0.0496$ sham versus RT1). In the hippocampus, we observed an increase of GFAP levels in sham-treated TgAD rats compared to WT animals without effect of LD-RT1 treatment (Fig. 2e and Supplementary Figure 2; One-way ANOVA, $F_{(2,21)} = 9.365$, $p = 0.002$; Tukey's multiple comparisons test: $p = 0.0027$ WT versus sham, $p = 0.0031$ WT versus RT1, $p = 0.9212$ sham versus RT1). The same pattern was measured for STAT3α (Fig. 2f; One-way ANOVA, $F_{(2,26)} = 5.179$, $p = 0.0128$; Tukey's multiple comparisons test: $p = 0.0120$ WT versus sham, $p = 0.6146$ WT versus RT1, $p = 0.0857$ sham versus RT1) and sCLU (Fig. 2 g; One-way ANOVA, $F_{(2,27)} = 13.35$, $p < 0.0001$; Tukey's multiple comparisons test: $p = 0.0007$ WT versus sham, $p = 0.0002$ WT versus RT1, $p = 0.9021$ sham versus RT1). However, SERPINA3 was unchanged between groups (Fig. 2 h). To go further, we used immunostaining to analyze the astrocyte reactivity in the different hippocampal subregions. A heterogeneous expression of GFAP was observed between subregions of the hippocampus in sham TgAD rats (Fig. 2i). Indeed, GFAP density (% $GFAP^+$ area) was significantly higher in the subiculum (sub) than in the ventral hippocampus (vH), and intermediate levels were measured in

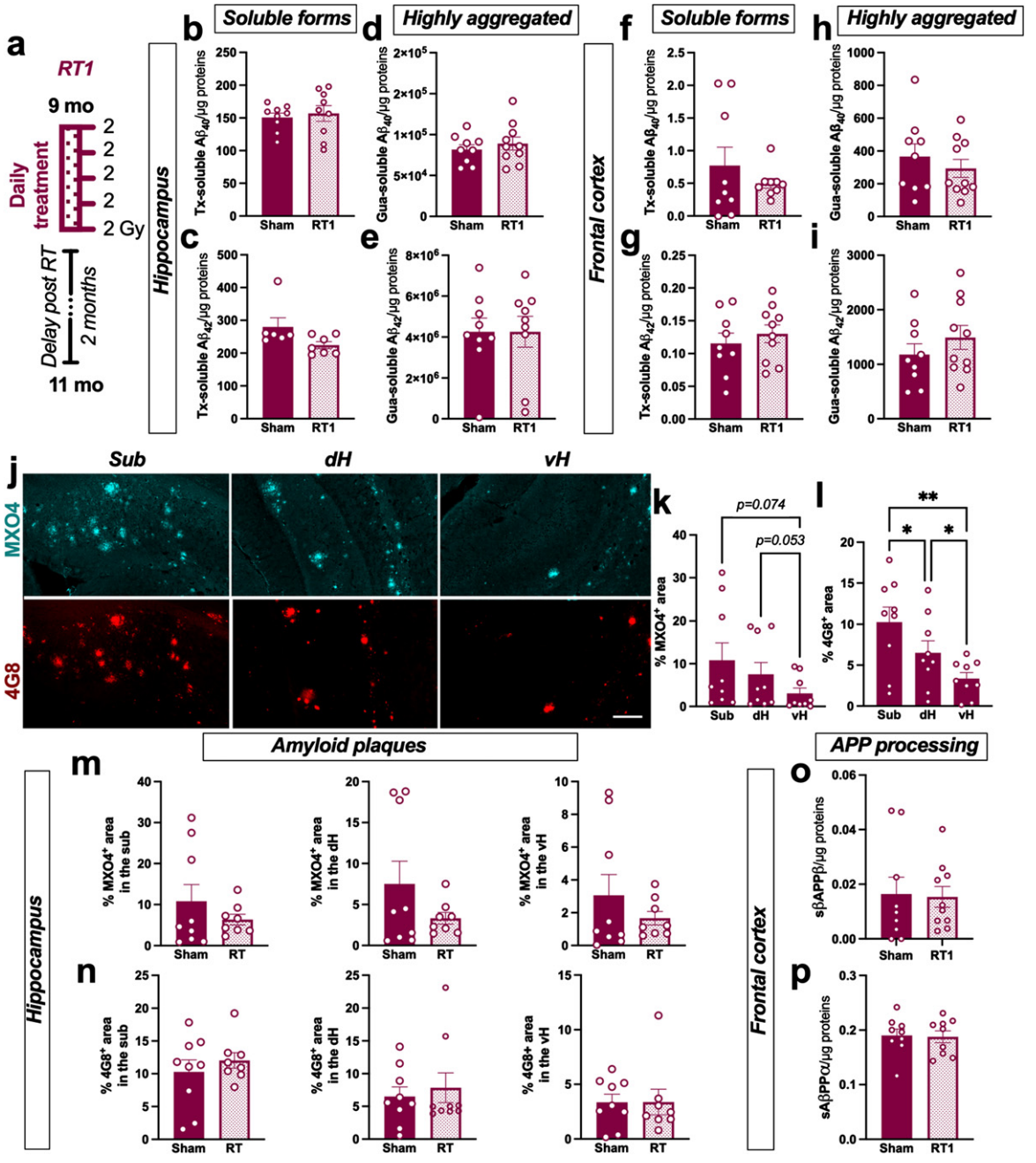

Fig. 1. **LD-RT does not reduce amyloid load in early AD females**. a) Female TgF344-AD were bilaterally treated by X-ray radiation (2 Gy × 5 fractions delivered daily; RT1) at 9-month-old, modeling an early AD stage, and analyzed 2 months later. Sham-treated TgAD rats and WT were only anesthetized. Concentration of $A\beta_{40}$ (b) and $A\beta_{42}$ (c) measured in the triton (Tx) soluble fraction of the hippocampus by ELISA. Concentration of $A\beta_{40}$ (d) and $A\beta_{42}$ (e) measured in Gua-soluble fraction of the hippocampus by ELISA. (f–i) Concentration of the different Aβ peptides in the frontal cortex by ELISA. (j) Representative images of amyloid plaques labelled with Methoxy-XO4 (MXO4; blue) or 4G8 antibody (red) in hippocampal subregions in a sham treated TgAD rat. Scale bar = 150 µm. Distribution of $MXO4^+$ (k) and $4G8^+$ (l) plaques in the hippocampal subregions (Sub, subiculum; dH, dorsal hippocampus; vH, ventral hippocampus) in sham animals. Quantification of $MXO4^+$ (m) and $4G8^+$ (n) plaques in the different hippocampal subregions in sham and RT1-treated rats. Concentration of sAβPPβ (o) and sAβPPα (p) in the Tx-soluble fraction of the frontal cortex measured by ELISA. Unpaired *t*-test or One-way ANOVA and Tukey's multiple comparisons test. $^*p < 0.005$, $^{**}p < 0.01$.

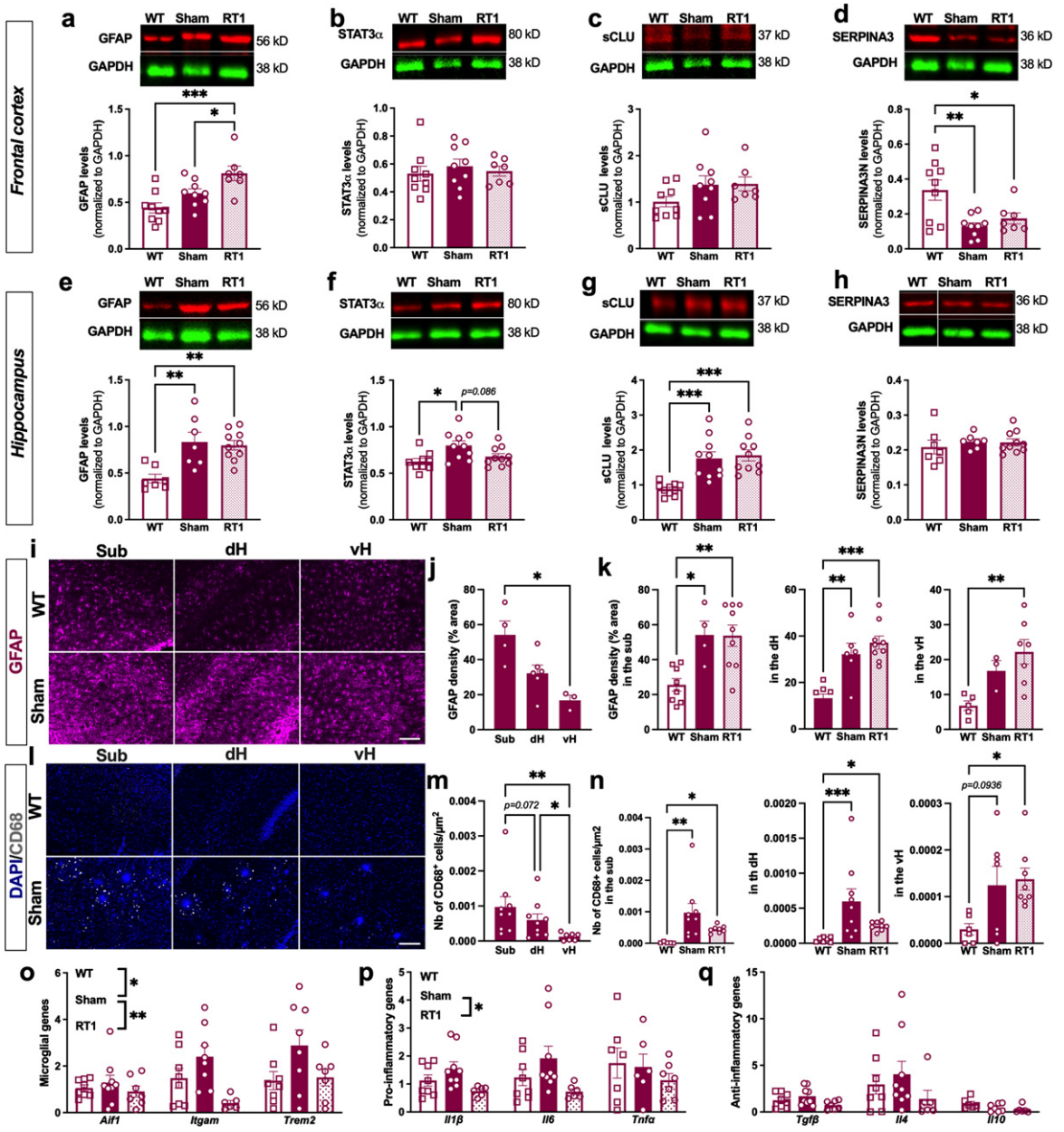

Fig. 2. **LD-RT reduces microglial inflammation markers in early AD females**. Quantification of astrocytic markers including GFAP (a), STAT3α (b), secreted CLUSTERIN (sCLU) (c), and SERPINA3 N (d) levels by western blot in the frontal cortex. Quantification of GFAP (e), STAT3α (f), secreted CLUSTERIN (sCLU) (g), and SERPINA3N (h) levels by western blot in the hippocampus. Data are normalized to GAPDH levels. One-way ANOVA and Tukey' multiple comparisons test. i) Representative images of GFAP (magenta) staining in the subiculum (sub), dorsal hippocampus (dH) and ventral hippocampus (vH) of WT and sham treated TgAD rats. Scale bar = 100 µm. j) Quantification of the GFAP density (% positively stained area) in the Sub, dH and vH in sham-treated TgAD rats. k) Quantification of the GFAP density (% positively stained area) in the different groups in the sub, dH and vH. l) Representative images of CD68 (grey; merged with DAPI in blue) staining in the sub, dH and vH of WT and sham treated TgAD rats. Scale bar = 100 µm. m) Quantification of the number of $CD68^+$ cells/μm^2 in sham-treated TgAD rats. n) Quantification of the number of $CD68^+$ cells/μm^2 in the different groups in the sub, dH and vH. One-way ANOVA and Tukey's multiple comparisons test or Kruskal-Wallis and Dunn's multiple comparisons test. (o–q) mRNA levels quantified by qPCR in the cortex of animals. Two-way ANOVA (group and gene as between factors) and Tukey's multiple comparisons test. # or $^*p < 0.05$, $^{**}p < 0.01$, $^{***}p < 0.001$.

the dorsal hippocampus (dH) (Fig. 2j; One-way-ANOVA, $F_{(1.315,3.287)} = 12.90$, $p = 0.0301$; Tukey's multiple comparisons test $p = 0.1119$ Sub versus dH, $p = 0.0404$ Sub versus vH, $p = 0.1507$ dH versus vH). A significant increase of GFAP density in the different subregions of the hippocampus was measured in sham-treated TgAD rats and in RT1-treated rats compared to WT (Fig. 2k; Sub: One-way ANOVA, $F_{(2,18)} = 8.567$, $p = 0.0024$; Tukey's multiple comparisons test: $p = 0.0172$ WT versus sham, $p = 0.0035$ WT versus RT1, $p = 0.9987$ sham versus RT1; dH: One-way ANOVA, $F_{(2,20)} = 18.41$, $p < 0.0001$; Tukey's multiple comparisons test: $p = 0.0013$ WT versus sham, $p < 0.0001$ WT versus RT1, $p = 0.5137$ sham versus RT1, vH: One-way ANOVA, $F_{(2,12)} = 6.898$, $p = 0.0101$; Tukey's multiple comparisons test: $p = 0.1744$ WT versus sham, $p = 0.0078$ WT versus RT1, $p = 0.5260$ sham versus RT1). Surprisingly, LD-RT1 did not reduce the astrocytic response (Fig. 2k).

Regarding microglial cells, we did not observe $CD68^+$ cells in the hippocampus of WT rats (Fig. 2l). However, a clear CD68 expression (number of $CD68^+$ cells/μm^2) was observed in sham-treated TgAD rats, mainly around amyloid plaques, showing also an inflammatory response from microglial cells in TgAD at an early AD stage (Fig. 2l). The number of $CD68^+$ cells/μm^2 was also differentially distributed within hippocampal subregions, with higher number of positive cells in the subiculum than in the dH than in the vH (Fig. 2m; One-way ANOVA, $F_{(1.148,8.038)} = 8.987$, $p = 0.0151$; Tukey's multiple comparisons test: $p = 0.0722$ Sub versus dH, $p = 0.0080$ Sub versus vH, $p = 0.0237$ dH versus vH). The overexpression of CD68 in sham-treated TgAD rats compared to WT was also validated. Interestingly, LD-RT1 seems to reduce this overexpression (Fig. 2n; Sub: Kruskal-Wallis, $p = 0.0004$; Dunn's multiple comparisons test: $p = 0.0014$ WT versus sham, $p = 0.0408$ WT versus RT1, $p = 0.7834$ sham versus RT1; dH: Kruskal-Wallis, $p = 0.0007$; Dunn's multiple comparisons test: $p = 0.0006$ WT versus sham, $p = 0.0153$ WT versus RT1, $p > 0.9999$ sham versus RT1; vH: One-way ANOVA, $F_{(2,18)} = 3.853$, $p = 0.0405$; Tukey's multiple comparisons test: $p = 0.0936$ WT versus sham, $p = 0.0441$ WT versus RT1, $p = 0.9401$ sham versus RT1). To further investigate a potential anti-inflammatory effect on microglial cells after LD-RT1, we performed qPCR in the cortex. The microglial response in TgAD rats was confirmed as demonstrated by the significant upregulation of microglial genes Aif1, Itgam and Trem2, but probably slight as there were no modulation of pro-(Il1β, Il6, Tnfα) or anti-inflammatory (Tgfβ, Il4, Il10) genes between those groups. Interestingly, LD-RT1 reduced the expression of microglial reactivity markers and pro-inflammatory genes, without affecting anti-inflammatory genes (Fig. 2o–q; Microglial genes: Two-way ANOVA, $F_{(2,64)} = 7.144$, $p = 0.0016$ for group main effect, $F_{(2,64)} = 3.566$, $p = 0.0340$ for gene main effect, $F_{(4,60)} = 1.535$, $p = 0.2037$ for group × gene interaction, Tukey's multiple comparisons test: $p = 0.0174$ WT versus sham, $p = 0.5278$ WT versus RT1, $p = 0.0010$ sham versus RT1; Pro-inflammatory genes: Two-way ANOVA, $F_{(2,57)} = 4.425$, $p = 0.0164$ for group main effect, $F_{(2,57)} = 0.8251$, $p = 0.4433$ for gene main effect, $F_{(4,57)} = 0.626$ $p = 0.7628$ for group × gene interaction, Tukey's multiple comparisons test: $p = 0.4420$ WT versus sham, $p = 0.1797$ WT versus RT1, $p = 0.0120$ sham versus RT1; Anti-inflammatory genes: Two-way ANOVA, $F_{(2,57)} = 2.073$, $p = 0.1351$ for group main effect, $F_{(2,57)} = 6.727$, $p = 0.0024$ for gene main effect, $F_{(4,57)} = 0.6915$, $p = 0.6009$ for group × gene interaction).

Altered fractionations did not induce an anti-amyloid effect in early AD females

Altered fractionations with lower doses or longer overall treatment time have demonstrated anti-inflammatory effects in peripheral pathologies. Consequently, to evaluate other treatment regimens that could increase the therapeutic effect, we also tested in early AD females the following schedules: one fraction of 2 Gy delivered once-a-week for 5 weeks (RT2) or with 10 fractions of 1 Gy delivered twice a week (RT3) (same total doses than RT1; Fig. 3a). First, we quantified the different concentrations in soluble or poorly aggregated forms of $A\beta_{40}$ and $A\beta_{42}$ (Fig. 3b, c) or the highly aggregated forms (Fig. 3d, e) in the hippocampus. However, as for LD-RT1 regimen, no effect was observed on $A\beta_{40}$ peptides or for $A\beta_{42}$ highly aggregated forms in RT2- or RT3-treated TgAD compared to sham-treated animals. Surprisingly, RT2 and RT3 regimens even significantly or tend to increase poorly aggregated forms of $A\beta_{42}$ compared to sham-treated animals (Fig. 3c; Kruskal-Wallis test, $p = 0.0234$, Dunn's multiple comparisons test: $p = 0.0338$ Sham versus RT2, $p = 0.0555$ Sham versus RT3, $p > 0.9999$ RT2 versus RT3). The same measurements were realized in the frontal cortex without differences, including for

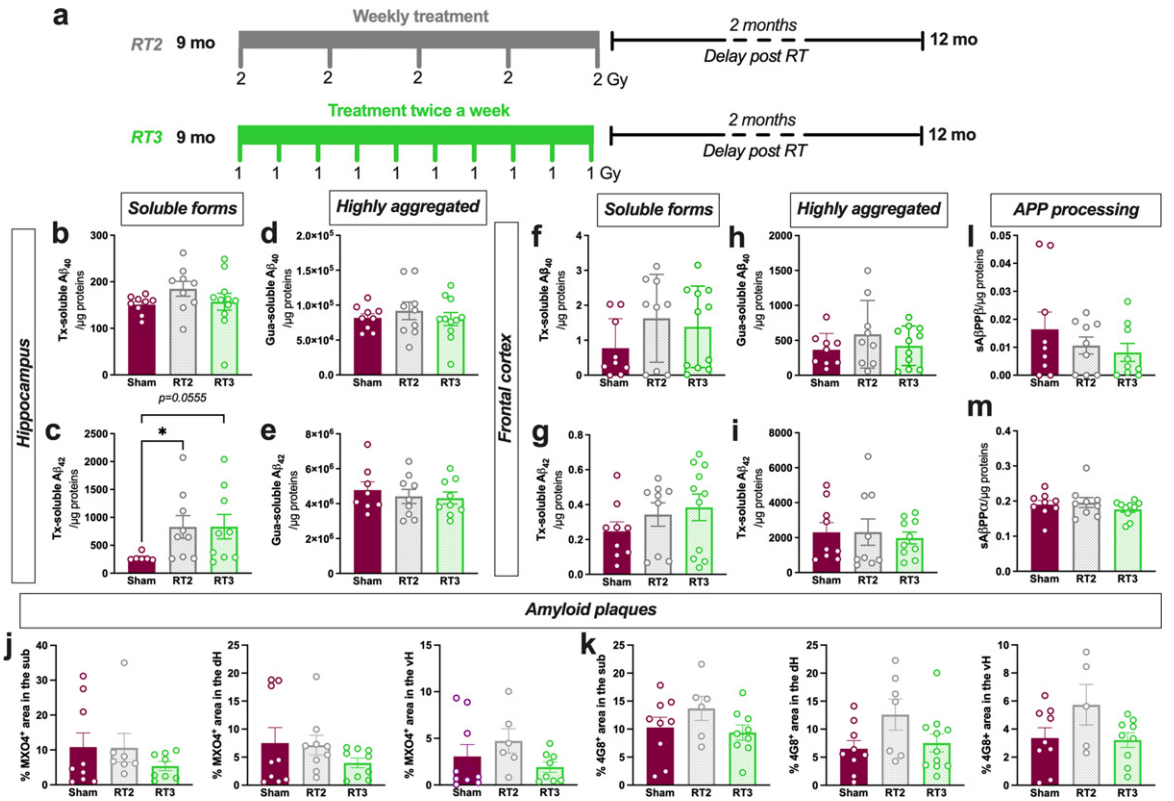

Fig. 3. **Altered fractionations of radiation do not improve anti-amyloid effects in females**. a) Female TgF344-AD rats were bilaterally treated by X-ray radiation (2 Gy × 5 fractions delivered once-a-week; RT2 or 1 Gy × 10 fractions delivered twice a week; RT3) at 9-month-old and analyzed 2 months later. Concentration of $A\beta_{40}$ (b) and $A\beta_{42}$ (c) measured in the triton (Tx) soluble fraction of the hippocampus by ELISA. Concentration of $A\beta_{40}$ (d) and $A\beta_{42}$ (e) measured in Gua-soluble fraction of the hippocampus by ELISA. (f–i) Concentration of different Aβ peptides in the frontal cortex by ELISA. Amyloid plaque density in the hippocampus stained using Methoxy-XO4 ($MXO4^+$; j) or 4G8 antibody (k). Concentration of sAβPPβ (l) and sAβPPα (m) in the Tx-soluble fraction of the frontal cortex measured by ELISA. One-way ANOVA or Kruskal-Wallis and Dunn's comparisons test. $^*p < 0.05$.

Tx-soluble Aβ42 peptides (Fig. 3f–i). The quantification of $MXO4^+$ plaque density (Fig. 3j) or $4G8^+$ plaque density (Fig. 3k) in the different subregions of the hippocampus reveals no effect of RT2 or RT3 regimens. The amyloidogenic (Fig. 3l) or the non-amyloidogenic (Fig. 3 m) pathways were not impacted by LD-RT treatments, showing that lower fractions did not differentially impact the amyloid load in early AD females.

Altered fractionations did not induce an anti-inflammatory effect in early AD females

Finally, we analyzed the astrocytic markers after LD-RT2 and LD-RT3 treatments. As in the other cohort, in the frontal cortex, no effect of LD-RT was observed whatever the treatment regimen studied (Fig. 4a–e and Supplementary Figure 3), and a reduction of SERPINA3 N was quantified in all TgAD cohorts compared to WT animals (Fig. 4e; One-way ANOVA, $F_{(3,29)} = 11.00$, $p < 0.0001$; Tukey's multiple comparisons test: $p = 0.0008$ WT versus sham, $p = 0.0003$ WT versus RT2, $p = 0.0004$ WT versus RT3). In the hippocampus, we did not observe any effect of treatments on GFAP, STAT3α, sCLU neither (Fig. 4f–j and Supplementary Figure 4). LD-RT2 only reduced SERPINA3N levels in the hippocampus (Fig. 4j; One-way ANOVA, $F_{(3,24)} = 3.595$, $p = 0.0282$; Tukey's multiple comparisons test: $p = 0.0336$ WT versus RT2). By immunohistology, we observed that GFAP density was not impacted by RT2 or RT3 schedules, whatever the subregion studied (Fig. 4k; Sub: One-way ANOVA, $F_{(3,22)} = 4.930$, $p = 0.0091$; Tukey's multiple comparisons test: $p = 0.0082$ WT versus sham, $p = 0.0844$ WT versus RT2, $p = 0.1348$ WT versus RT3, $p = 0.6728$ sham versus RT2, $p = 0.2920$ sham versus RT3, $p = 0.9328$ RT2 versus RT3; dH: One-

way ANOVA, $F_{(3,25)} = 7.019$, $p = 0.0014$; Tukey's multiple comparisons test: $p = 0.0144$ WT versus sham, $p = 0.0083$ WT versus RT2, $p = 0.0022$ WT versus RT3, $p = 0.9965$ sham versus RT2, $p = 0.9831$ sham versus RT3, $p = 0.9992$ RT2 versus RT3; vH: One-way ANOVA, $F_{(3,15)} = 3.062$, $p = 0.0605$).

We also investigated the microglial response in the hippocampal subregions after each treatment. LD-RT2 or LD-RT3 did not influence the number of $CD68^+$ cells/μm^2, except in the vH where an increase of microglial reactivity was observed in RT2-treated rats compared to other groups, showing that both LD-RT regimens were not efficient to decrease microglial response in 9-month-old females (Fig. 4l; Sub: Kruskal-Wallis, $p = 0.0090$; Dunn's multiple comparisons test: $p = 0.0126$ WT versus sham, $p = 0.1406$ WT versus RT2, $p = 0.0171$ WT versus RT3, $p > 0.9999$ sham versus RT2, $p > 0.9999$ sham versus RT3, $p > 0.9999$ RT2 versus RT3; dH: Kruskal-Wallis, $p = 0.0011$; Dunn's multiple comparisons test: $p = 0.0053$ WT versus sham, $p = 0.0012$ WT versus RT2, $p = 0.0360$ WT versus RT3, $p > 0.9999$ sham versus RT2, $p > 0.9999$ sham versus RT3, $p > 0.9999$ RT2 versus RT3; vH: One-way ANOVA, $F_{(3,25)} = 13.03$, $p < 0.0001$; Tukey's multiple comparisons test: $p = 0.5355$ WT versus sham, $p < 0.0001$ WT versus RT2, $p = 0.5831$ WT versus RT3, $p = 0.0009$ sham versus RT2, $p = 0.9993$ sham versus RT3, $p = 0.0005$ RT2 versus RT3). qPCR analyses in the cortex of animals even suggest an induction of a slight inflammatory response by RT3 (Fig. 4m–o, Microglial genes: Two-way ANOVA, $F_{(3,96)} = 7.961$, $p < 0.0001$ for group main effect, $F_{(2,96)} = 4.023$, $p = 0.0210$ for gene main effect, $F_{(6,96)} = 1.072$, $p = 0.3845$ for group × gene interaction, Tukey's multiple comparisons test: $p = 0.2179$ WT versus sham, $p = 0.6165$ WT versus RT2, $p < 0.0001$ WT versus RT3, $p = 0.8946$ sham versus RT2, $p = 0.0394$ sham versus RT3, $p = 0.0057$ RT2 versus RT3; Pro-inflammatory genes: Two-way ANOVA, $F_{(3,94)} = 3.345$, $p = 0.0224$ for group main effect, $F_{(2,94)} = 1.894$, $p = 0.1562$ for gene main effect, $F_{(6,94)} = 1.888$, $p = 0.0908$ for group × gene interaction, Tukey's multiple comparisons test: $p > 0.9999$ WT versus sham, $p > 0.9999$ WT versus RT2, $p = 0.0664$ WT versus RT3, $p > 0.9999$ sham versus RT2, $p = 0.0778$ sham versus RT3, $p = 0.0646$ RT2 versus RT3; Anti-inflammatory genes: Two-way ANOVA, $F_{(3,93)} = 2.070$, $p = 0.1095$ for group main effect, $F_{(2,93)} = 14.82$, $p < 0.0001$ for gene main effect, $F_{(6,93)} = 2.138$, $p = 0.0562$ for group × gene interaction).

To see if astrocyte and microglial reactivity were associated with the $MXO4^+$ or $4G8^+$ plaques in the whole hippocampus, correlation analyses were performed. The GFAP density was not correlated with the % $MXO4^+$ plaques (Fig. 4p; Pearson coefficient $r = 0.181$, $p = 0.135$) but tend to be positively associated with the % $4G8^+$ plaques in the hippocampus (Fig. 4q; $r = 0.243$, $p = 0.051$). However, the number of $CD68^+$ cells/μm^2 was positively correlated with both amount of $MXO4^+$ plaques (Fig. 4r; $r = 0.631$, $p < 0.001$) and $4G8^+$ plaques (Fig. 4s; $r = 0.511$, $p < 0.001$).

No behavioral alteration in early AD females

The early timepoint of treatment was validated using classical behavioral tests, including the alternative Y maze to assess the spatial working memory and the open flied test to quantify the general locomotion. No difference was measured between WT and TgAD rats and none of the treatments influenced behavioral performances of animals (Fig. 5a, b).

DISCUSSION

Low-dose radiation therapy has demonstrated encouraging results in different mouse and rat models on amyloid load, neuroinflammation [7–13] and on cognition [10]. Here, we evaluate the effect of three regimens in 9-month-old female TgAD, including one regimen having previously shown effectiveness in male animals of the same model and age. The first regimen (named RT1 in the present study) did not influence amyloid load but reduced microglial-inflammatory markers without affecting astrocytes. Altered fractionations with longer overall treatment time, showing interesting anti-inflammatory properties in peripheral pathologies [15, 20] (RT2, RT3 regimens), were unable to reduce inflammation markers or amyloid load.

The number of studies evaluating the effect of LD-RT is rapidly increasing, but the regimens, the age of treatment and the delay post LD-RT are variable making difficult to define the most efficient protocol, and sex as possible influencing variable has been neglected. In a previous study, we demonstrated that a reference regimen of LD-RT (2 Gy × 5 fractions delivered daily) significantly reduced all forms of amyloid peptides (soluble and highly aggregated forms) in addition to reduced inflammation markers in male TgAD rats at the same age [14]. However, the effects were lower or even not observed in female

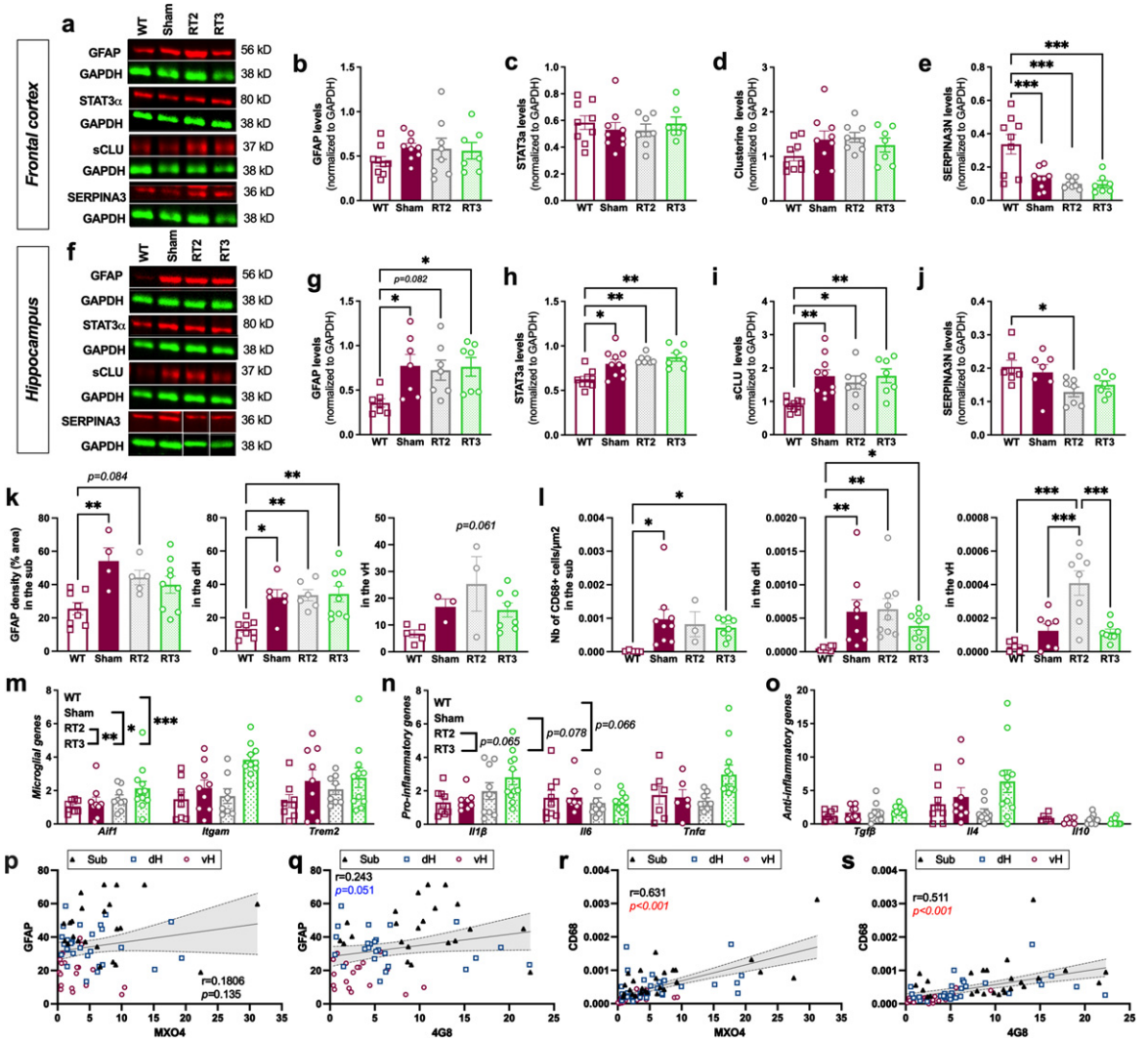

Fig. 4. **Altered fractionations of radiation do not reduce inflammation markers in females**. (a) Representative western blot images in the frontal cortex. Quantification of GFAP (b), STAT3α (c), secreted CLUSTERIN (sCLU) (d), and SERPINA3N (e) levels by western blot in the frontal cortex. (f) Representative western blot images in the hippocampus. Quantification of GFAP (g), STAT3α (h), sCLU (i), and SERPINA3N (j) levels by western blot in the hippocampus. Data are normalized to GAPDH levels. One-way ANOVA and Tukey's multiple comparisons test. (k) Quantification of the GFAP density (% positively stained area) in the subiculum (sub), dorsal hippocampus (dH) and ventral hippocampus (vH) in the different groups. (l) Quantification of the number of $CD68^+$ cells/μm^2 in the hippocampal subregions. One-way ANOVA and Tukey's multiple comparison test or Kruskal-Wallis and Dunn's multiple comparisons test. (m–o) mRNA levels quantified by qPCR in the cortex of animals. Two-way ANOVA (group and gene as between factors) and Tukey's multiple comparison test. Correlation of GFAP density and % of $MXO4^+$ plaques (p) or % of $4G8^+$ plaques (q) in the entire hippocampus. Correlation of the number of $CD68^+$ cells/μm^2 and the % of $MXO4^+$ plaques (r) or the % of $4G8^+$ plaques (s) in the entire hippocampus. Different symbols represent the subregions (Sub = magenta; dH = blue; vH = black). The Pearson coefficient (r) and the *p* value are indicated for the entire hippocampus. $^*p < 0.05$, $^{**}p < 0.01$, $^{***}p < 0.001$.

3xTg-AD mice also treated at an early stage of the disease [12]. For this reason, we designed a study to replicate the experiment, proven to be effective in male animals, in 9-month-old female TgAD rats.

Using a classical behavioral test to assess spatial memory alteration, we validated that the study was realized at an early stage of the disease as both genotypes successfully explored the Y maze. The age of behavioral alteration onset is not consistent between studies in TgAD rats. Indeed, some studies described early learning and/or memory alterations at the age of 4 [21], 9–12 [16, 22–26], 15 [16], and 24 [16,

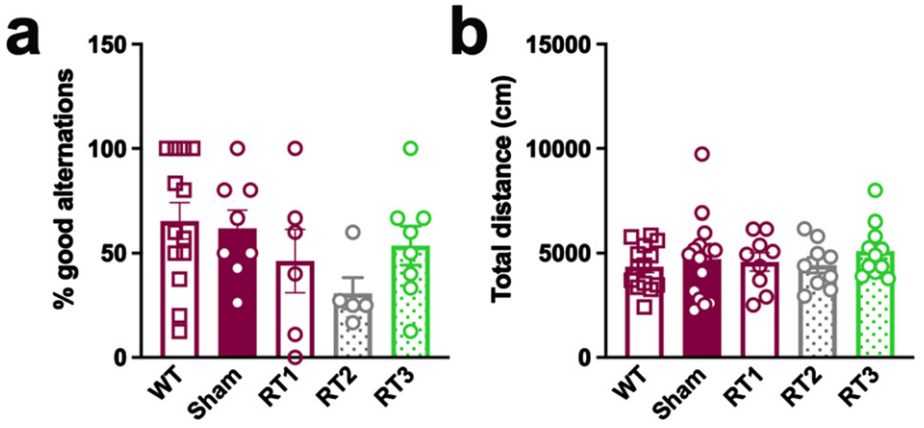

Fig. 5. **LD-RT does not influence behavioral performances of TgAD rats**. (a) The spatial working memory of rats was assessed 2 months after the last session of LD-RT using the alternative Y maze test. One-way ANOVA. (b) Quantification of the general locomotion of animals in the open field after LD-RT. Kruskal-Wallis test.

24] months or impaired reversal learning at 6 months [27], whereas other did not report any difference compared to WT animals at 4–6 [23, 28–30], 7–11 [23], 13 [30], 15–18 [31], and 24 [31, 32] months of age. Consequently, based on our results and the literature, we presumably model an early AD stage.

We investigated the effect of this regimen (RT1) on the different forms of amyloid peptides. Neither the soluble or poorly aggregated forms or the most aggregated forms of $A\beta_{40}$ and $A\beta_{42}$ were impacted in the females, contrary to males [14]. The absence of effect was also measured on amyloid plaques of the hippocampus. Moreover, the density of amyloid plaques does not seem to influence the treatment response as no effect was observed in the dorsal or the ventral hippocampus, showing fewer amyloid plaques than the subiculum, as already demonstrated in this model at the same age [22]. In young males, we described for the first time a stimulation of the non-amyloidogenic pathway, demonstrated by the increased levels of sAβPPα, without modulation of the amyloid production [14]. In females, neither the sAβPPα nor the sAβPPβ was modulated by LD-RT. These results clearly suggest a different response of males and females to irradiation. This difference may be due to a more advanced pathology in females than in males, leading to pathological process too deeply rooted to be reversed or significantly halted. Indeed, the sex effect in AD, with an enhanced pathology hallmarks in females, is commonly described in other AD mouse models [33–35] and some studies suggest also this difference in TgAD rats [23, 36, 37]. Further studies are consequently needed to validate this difference in our model on the different amyloid peptides studied. Unfortunately, lower fractionations did not change the treatment response of females as we did not observe any modulation of amyloid peptides or plaques in the hippocampus or in the frontal cortex. However, some pathological processes seem to start earlier in male than in female TgAD rats (i.e., alterations in basal transmission at the CA3-CA1 synapses) [38], and studying the sex-specific effect of LD-RT using those outcomes could also help to refine those assumptions.

When evaluating the effect on neuroinflammation, a minor effect could also be observed in females. The presence of reactive astrocytes and reactive microglial cells was measured before the appearance of clear cognitive symptoms, highlighting the early role of glial cells in AD pathogenesis. This observation is consistent with the literature [39, 40]. We also observed a differential repartition of reactive astrocytes and $CD68^+$ microglial cells in the subregions of the hippocampus. The heterogeneity of reactive microglia is consistent with the distribution of amyloid plaques in the hippocampus as shown by the positive correlation between the number of reactive microglia $CD68^+$ cells and diffuse and dense-core plaques ($MXO4^+$ and $4G8^+$ plaques). Interestingly, reactive astrocytes seem only to be correlated with the amount of $4G8^+$ plaques, suggesting that astrocytes are more sensitive to diffuse plaques. LD-RT1 did not reduce GFAP levels, which is consistent with our finding in young male TgAD [14]. However, at the contrary to males, no effect was observed on sCLU neither. The same results were obtained for the two other treatment schedules. Regarding microglial cells, the reduction of the expression lev-

els of microglial genes and pro-inflammatory genes evidenced an anti-inflammatory effect of LD-RT1. These results suggest that microglial cells are more sensitive to radiation than astrocytes in females. Surprisingly, the effect was not observed for lower fractionations, which even worsened the inflammatory response.

Overall, these data suggest a different response of males and females to radiation therapy with an anti-amyloid and strong anti-inflammatory effect in males whereas LD-RT1 reduced only microglial response in females at an early stage of the pathology. As our investigation in males and females was performed in separate sessions, we cannot directly compare the data, as the specific experimental conditions might impact the quantification obtained even when all other parameters are controlled. A complementary study, performing the same experiments in animals of both sexes for those metrics, would allow to validate this hypothesis. It is important to note that both male and female TgAD rats did not display cognitive alterations before treatment at 9-month-old (Supplementary Figure 5). If the sex-specific effects of LD-RT are confirmed, it would also underscore that the anti-amyloid effect observed in males was not directly related to the reduction of inflammation but that those responses are, at least in part, two separate processes.

Sex hormones, such as estrogens, testosterone, and progesterone seem to play an important role in inflammation and oxidative stress regulation [41], two important processes observed in neurodegenerative diseases including AD. The loss of estrogen during aging and with menopause is one of the major hypotheses to explain the increased risk factor for AD in women. Moreover, testosterone could be directly involved in neuroprotective mechanism against AD, participating to Aβ processing reduction and indirect degradation as examples [42–45]. Androgen deprivation therapy, classically used for the treatment of high-risk and locally advanced prostate cancer, is suspected to increase the risk of AD [46]. In the brain, sex hormones could act on the astrocytic and microglial response in inflammatory conditions. For example, a supplementation in testosterone or in estradiol reduced astrocyte and microglial reactivity in a model of brain injury [47]. Estradiol could also favor the M2 microglial cell population [48], an extreme class of activated microglial displaying neuroprotective properties. If sex hormones influence glial cell response to an injury, we may hypothesize that they will not react the same way to radiation exposure in the AD pathological context. Further studies must investigate these hypotheses.

Finally, in a previous study, we evaluated the LD-RT1 and LD-RT2 regimens on old female TgAD, showing an advanced pathology (high amyloid load, neuroinflammation, and cognitive deficits). The LD-RT1 schedule efficiently improved spatial memory of treated rats, without modulation of amyloid load or neuroinflammation markers [10]. This result suggests that females could also positively respond to LD-RT, but not on the same pathological outcomes, and supposes different mechanisms of actions in both sexes. Other studies are consequently necessary to see if the cognitive restoration is also observed in old males, as well as the anti-amyloid and anti-inflammatory effects, given that cognitive restoration is obviously the ultimate objective of the application of a treatment.

Conclusion

Overall, LD-RT induces only a reduction of the microglial-mediated inflammation without impacting the amyloid load, contrary to the results obtained in our previous study at the same age in males. This study suggests a sex effect in the treatment response in term of amyloid and inflammation. More studies have to be performed to understand this dichotomy and to identify mechanisms involved in the treatment response in 9-month-old male TgAD rats. Particular attention should be paid in ongoing pilot clinical trials including sex as variable for the evaluation of treatment effectiveness.

AUTHOR CONTRIBUTIONS

Kelly Ceyzériat (Conceptualization; Formal analysis; Investigation; Supervision; Visualization; Writing – original draft); Emma Jaques (Investigation; Writing – review & editing); Yesica Gloria (Investigation; Writing – review & editing); Aurélien Badina (Investigation; Writing – review & editing); Philippe Millet (Writing – review & editing); Nikolaos Koutsouvelis (Methodology; Writing – review & editing); Giovanna Dipasquale (Methodology; Writing – review & editing); Giovanni B. Frisoni (Writing – review & editing); Thomas Zilli (Conceptualization; Funding acquisition; Supervision; Writing – original draft); Valentina Garibotto (Conceptualization; Funding acquisition; Supervision; Writing – original draft); Benjamin Tournier (Conceptualization; Formal analysis; Funding acqui-

sition; Investigation; Supervision; Writing – original draft).

ACKNOWLEDGMENTS

Pia Lovero, Maria Surini, Arthur Paquis, and William Harris for the technical assistance. We thank all the team of the radiation-oncology division, Geneva University Hospitals, for its help with the radiation treatments of animals. Authors also thank the Rat Resource and Research Center (RRRC, Columbia) for providing the rat model.

FUNDING

This work was supported by the Velux foundation (grant number 1123).

CONFLICT OF INTEREST

The authors have no conflict of interest to report.

DATA AVAILABILITY

The data supporting the findings of this study are available on request from the corresponding author.

SUPPLEMENTARY MATERIAL

The supplementary material is available in the electronic version of this article: https://dx.doi.org/10.3233/JAD-231153.

REFERENCES

[1] Dar NJ, Glazner GW (2020) Deciphering the neuroprotective and neurogenic potential of soluble amyloid precursor protein alpha (sAPPα). *Cell Mol Life Sci* **77**, 2315-2330.

[2] Ben Haim L, Carrillo-de Sauvage M-A, Ceyzériat K, Escartin C (2015) Elusive roles for reactive astrocytes in neurodegenerative diseases. *Front Cell Neurosci* **9**, 278.

[3] Leng F, Edison P (2021) Neuroinflammation and microglial activation in Alzheimer disease: Where do we go from here? *Nat Rev Neurol* **17**, 157-172.

[4] Monterey MD, Wei H, Wu X, Wu JQ (2021) The many faces of astrocytes in Alzheimer's disease. *Front Neurol* **12**, 619626.

[5] Ferretti MT, Iulita MF, Cavedo E, Chiesa PA, Schumacher Dimech A, Santuccione Chadha A, Baracchi F, Girouard H, Misoch S, Giacobini E, Depypere H, Hampel H, Women's Brain Project and the Alzheimer Precision Medicine Initiative (2018) Sex differences in Alzheimer disease – the gateway to precision medicine. *Nat Rev Neurol* **14**, 457-469.

[6] Buckley RF, Gong J, Woodward M (2023) A call to action to address sex differences in Alzheimer disease clinical trials. *JAMA Neurol* **80**, 769-770.

[7] Marples B, McGee M, Callan S, Bowen SE, Thibodeau BJ, Michael DB, Wilson GD, Maddens ME, Fontanesi J, Martinez AA (2016) Cranial irradiation significantly reduces beta amyloid plaques in the brain and improves cognition in a murine model of Alzheimer's disease (AD). *Radiother Oncol* **118**, 43-51.

[8] Wilson GD, Wilson TG, Hanna A, Fontanesi G, Kulchycki J, Buelow K, Pruetz BL, Michael DB, Chinnaiyan P, Maddens ME, Martinez AA, Fontanesi J (2020) Low dose brain irradiation reduces amyloid-β and tau in 3xTg-AD mice. *J Alzheimers Dis* **75**, 15-21.

[9] Kim S, Chung H, Ngoc Mai H, Nam Y, Shin SJ, Park YH, Chung MJ, Lee JK, Rhee HY, Jahng G-H, Kim Y, Lim YJ, Kong M, Moon M, Chung WK (2020) Low-dose ionizing radiation modulates microglia phenotypes in the models of Alzheimer's disease. *Int J Mol Sci* **21**, 4532.

[10] Ceyzériat K, Zilli T, Fall AB, Millet P, Koutsouvelis N, Dipasquale G, Frisoni GB, Tournier BB, Garibotto V (2021) Treatment by low-dose brain radiation therapy improves memory performances without changes of the amyloid load in the TgF344-AD rat model. *Neurobiol Aging* **103**, 117-127.

[11] Yang E-J, Kim H, Choi Y, Kim HJ, Kim JH, Yoon J, Seo Y-S, Kim H-S (2021) Modulation of neuroinflammation by low-dose radiation therapy in an animal model of Alzheimer's disease. *Int J Radiat Oncol Biol Phys* **111**, 658-670.

[12] Ceyzériat K, Tournier BB, Millet P, Dipasquale G, Koutsouvelis N, Frisoni GB, Garibotto V, Zilli T (2022) Low-dose radiation therapy reduces amyloid load in young 3xTg-AD mice. *J Alzheimers Dis* **86**, 641-653.

[13] Kim S, Nam Y, Kim C, Lee H, Hong S, Kim HS, Shin SJ, Park YH, Mai HN, Oh S-M, Kim KS, Yoo D-H, Chung WK, Chung H, Moon M (2020) Neuroprotective and anti-inflammatory effects of low-moderate dose ionizing radiation in models of Alzheimer's disease. *Int J Mol Sci* **21**, E3678.

[14] Ceyzériat K, Zilli T, Millet P, Koutsouvelis N, Dipasquale G, Fossey C, Cailly T, Fabis F, Frisoni GB, Garibotto V, Tournier BB (2022) Low-dose brain irradiation normalizes TSPO and CLUSTERIN levels and promotes the non-amyloidogenic pathway in pre-symptomatic TgF344-AD rats. *J Neuroinflammation* **19**, 311.

[15] Kriz J, Seegenschmiedt HM, Bartels A, Micke O, Muecke R, Schaefer U, Haverkamp U, Eich HT (2018) Updated strategies in the treatment of benign diseases-a patterns of care study of the german cooperative group on benign diseases. *Adv Radiat Oncol* **3**, 240-244.

[16] Cohen RM, Rezai-Zadeh K, Weitz TM, Rentsendorj A, Gate D, Spivak I, Bholat Y, Vasilevko V, Glabe CG, Breunig JJ, Rakic P, Davtyan H, Agadjanyan MG, Kepe V, Barrio JR, Bannykh S, Szekely CA, Pechnick RN, Town T (2013) A transgenic alzheimer rat with plaques, tau pathology, behavioral impairment, oligomeric Aβ, and frank neuronal loss. *J Neurosci* **33**, 6245-6256.

[17] Koutsouvelis N, Rouzaud M, Dubouloz A, Nouet P, Jaccard M, Garibotto V, Tournier BB, Zilli T, Dipasquale G (2020) 3D printing for dosimetric optimization and quality assurance in small animal irradiations using megavoltage X-rays. *Z Med Phys* **30**, 227-235.

[18] Serrano-Pozo A, Frosch MP, Masliah E, Hyman BT (2011) Neuropathological alterations in Alzheimer disease. *Cold Spring Harb Perspect Med* **1**, a006189.

[19] Alafuzoff I, Pikkarainen M, Arzberger T, Thal DR, Al-Sarraj S, Bell J, Bodi I, Budka H, Capetillo-Zarate E, Ferrer I, Gelpi E, Gentleman S, Giaccone G, Kavantzas N, King A, Korkolopoulou P, Kovács GG, Meyronet D, Monoranu C, Parchi P, Patsouris E, Roggendorf W, Stadelmann C, Streichenberger N, Tagliavini F, Kretzschmar H (2008) Inter-laboratory comparison of neuropathological assessments of beta-amyloid protein: A study of the BrainNet Europe consortium. *Acta Neuropathol* **115**, 533-546.

[20] Arenas M, Sabater S, Hernández V, Rovirosa A, Lara PC, Biete A, Panés J (2012) Anti-inflammatory effects of low-dose radiotherapy. Indications, dose, and radiobiological mechanisms involved. *Strahlenther Onkol* **188**, 975-981.

[21] Fowler CF, Goerzen D, Devenyi GA, Madularu D, Chakravarty MM, Near J (2022) Neurochemical and cognitive changes precede structural abnormalities in the TgF344-AD rat model. *Brain Commun* **4**, fcac072.

[22] Tournier BB, Barca C, Fall AB, Gloria Y, Meyer L, Ceyzériat K, Millet P (2021) Spatial reference learning deficits in absence of dysfunctional working memory in the TgF344-AD rat model of Alzheimer's disease. *Genes Brain Behav* **20**, e12712.

[23] Berkowitz LE, Harvey RE, Drake E, Thompson SM, Clark BJ (2018) Progressive impairment of directional and spatially precise trajectories by TgF344-Alzheimer's disease rats in the Morris Water Task. *Sci Rep* **8**, 16153.

[24] Morrone CD, Bazzigaluppi P, Beckett TL, Hill ME, Koletar MM, Stefanovic B, McLaurin J (2020) Regional differences in Alzheimer's disease pathology confound behavioural rescue after amyloid-β attenuation. *Brain* **143**, 359-373.

[25] Proskauer Pena SL, Mallouppas K, Oliveira AMG, Zitricky F, Nataraj A, Jezek K (2021) Early spatial memory impairment in a double transgenic model of Alzheimer's disease TgF-344 AD. *Brain Sci* **11**, 1300.

[26] Srivastava H, Lasher AT, Nagarajan A, Sun LY (2023) Sexual dimorphism in the peripheral metabolic homeostasis and behavior in the TgF344-AD rat model of Alzheimer's disease. *Aging Cell* **22**, e13854.

[27] Rorabaugh JM, Chalermpalanupap T, Botz-Zapp CA, Fu VM, Lembeck NA, Cohen RM, Weinshenker D (2017) Chemogenetic locus coeruleus activation restores reversal learning in a rat model of Alzheimer's disease. *Brain* **140**, 3023-3038.

[28] Koulousakis P, van den Hove D, Visser-Vandewalle V, Sesia T (2020) Cognitive improvements after intermittent deep brain stimulation of the nucleus basalis of Meynert in a transgenic rat model for Alzheimer's disease: A preliminary approach. *J Alzheimers Dis* **73**, 461-466.

[29] Bernaud VE, Bulen HL, Peña VL, Koebele SV, Northup-Smith SN, Manzo AA, Valenzuela Sanchez M, Opachich Z, Ruhland AM, Bimonte-Nelson HA (2022) Task-dependent learning and memory deficits in the TgF344-AD rat model of Alzheimer's disease: Three key timepoints through middle-age in females. *Sci Rep* **12**, 14596.

[30] Bac B, Hicheri C, Weiss C, Buell A, Vilcek N, Spaeni C, Geula C, Savas JN, Disterhoft JF (2022) The TgF344-AD rat: Behavioral and proteomic changes associated with aging and protein expression in a transgenic rat model of Alzheimer's disease. *Neurobiol Aging* **123**, 98-110.

[31] Voorhees JR, Remy MT, Cintrón-Pérez CJ, El Rassi E, Khan MZ, Dutca LM, Yin TC, McDaniel LN, Williams NS, Brat DJ, Pieper AA (2018) (–)-P7C3-S243 protects a rat model of Alzheimer's disease from neuropsychiatric deficits and neurodegeneration without altering amyloid deposition or reactive glia. *Biol Psychiatry* **84**, 488-498.

[32] Voorhees JR, Remy MT, Erickson CM, Dutca LM, Brat DJ, Pieper AA (2019) Occupational-like organophosphate exposure disrupts microglia and accelerates deficits in a rat model of Alzheimer's disease. *NPJ Aging Mech Dis* **5**, 3.

[33] Carroll JC, Rosario ER, Kreimer S, Villamagna A, Gentzschein E, Stanczyk FZ, Pike CJ (2010) Sex differences in β-amyloid accumulation in 3xTg-AD mice: Role of neonatal sex steroid hormone exposure. *Brain Res* **1366**, 233-245.

[34] Callahan MJ, Lipinski WJ, Bian F, Durham RA, Pack A, Walker LC (2001) Augmented senile plaque load in aged female beta-amyloid precursor protein-transgenic mice. *Am J Pathol* **158**, 1173-1177.

[35] Dennison JL, Ricciardi NR, Lohse I, Volmar C-H, Wahlestedt C (2021) Sexual dimorphism in the 3xTg-AD mouse model and its impact on pre-clinical research. *J Alzheimers Dis* **80**, 41-52.

[36] Chaudry O, Ndukwe K, Xie L, Serrano PA, Figueiredo-Pereira ME, Rockwell P (2022) Females outperform males in spatial learning despite increased amyloid plaques and microgliosis in a TgF344-AD rat model of Alzheimer's disease. *Sci Rep* **12**, 19129.

[37] Saré RM, Cooke SK, Krych L, Zerfas PM, Cohen RM, Smith CB (2020) Behavioral phenotype in the TgF344-AD rat model of Alzheimer's disease. *Front Neurosci* **14**, 601.

[38] Smith LA, McMahon LL (2018) Deficits in synaptic function occur at medial perforant path-dentate granule cell synapses prior to Schaffer collateral-CA1 pyramidal cell synapses in the novel TgF344-Alzheimer's disease rat model. *Neurobiol Dis* **110**, 166-179.

[39] Carter SF, Scholl M, Almkvist O, Wall A, Engler H, Langstrom B, Nordberg A (2012) Evidence for astrocytosis in prodromal Alzheimer disease provided by 11C-deuterium-L-deprenyl: A multitracer PET paradigm combining 11C-Pittsburgh compound B and 18F-FDG. *J Nucl Med* **53**, 37-46.

[40] Hamelin L, Lagarde J, Dorothée G, Leroy C, Labit M, Comley RA, de Souza LC, Corne H, Dauphinot L, Bertoux M, Dubois B, Gervais P, Colliot O, Potier MC, Bottlaender M, Sarazin M, Clinical IMABio3 team (2016) Early and protective microglial activation in Alzheimer's disease: A prospective study using 18F-DPA-714 PET imaging. *Brain* **139**, 1252-1264.

[41] Zárate S, Stevnsner T, Gredilla R (2017) Role of estrogen and other sex hormones in brain aging. Neuroprotection and DNA repair. *Front Aging Neurosci* **9**, 430.

[42] Ramsden M, Nyborg AC, Murphy MP, Chang L, Stanczyk FZ, Golde TE, Pike CJ (2003) Androgens modulate beta-amyloid levels in male rat brain. *J Neurochem* **87**, 1052-1055.

[43] Rosario ER, Carroll JC, Oddo S, LaFerla FM, Pike CJ (2006) Androgens regulate the development of neuropathology in a triple transgenic mouse model of Alzheimer's disease. *J Neurosci* **26**, 13384-13389.

[44] Yao M, Nguyen T-VV, Rosario ER, Ramsden M, Pike CJ (2008) Androgens regulate neprilysin expression: Role in reducing beta-amyloid levels. *J Neurochem* **105**, 2477-2488.

[45] McAllister C, Long J, Bowers A, Walker A, Cao P, Honda S-I, Harada N, Staufenbiel M, Shen Y, Li R (2010) Genetic targeting aromatase in male amyloid precursor protein transgenic mice down-regulates beta-secretase (BACE1) and prevents Alzheimer-like pathology and cognitive impairment. *J Neurosci* **30**, 7326-7334.

[46] Achard V, Ceyzériat K, Tournier BB, Frisoni GB, Garibotto V, Zilli T (2021) Biomarkers to evaluate androgen deprivation therapy for prostate cancer and risk of Alzheimer's disease and neurodegeneration: Old drugs, new concerns. *Front Oncol* **11**, 734881.

[47] Barreto G, Veiga S, Azcoitia I, Garcia-Segura LM, Garcia-Ovejero D (2007) Testosterone decreases reactive astroglia and reactive microglia after brain injury in male rats: Role of its metabolites, oestradiol and dihydrotestosterone. *Eur J Neurosci* **25**, 3039-3046.

[48] Habib P, Beyer C (2015) Regulation of brain microglia by female gonadal steroids. *J Steroid Biochem Mol Biol* **146**, 3-14.